

**Topological and magnetic phase transitions in  $\text{Bi}_2\text{Se}_3$  thin films with magnetic impurities**Hosub Jin,<sup>\*</sup> Jino Im,<sup>†</sup> and Arthur J. Freeman*Department of Physics and Astronomy, Northwestern University, Evanston, Illinois 60208, USA*

(Received 21 September 2011; published 11 October 2011)

When topological insulators meet broken time-reversal symmetry, they bring forth many novel phenomena, such as topological magnetoelectric, half-quantum Hall, and quantum anomalous Hall effects. From the well-known quantum spin Hall state in  $\text{Bi}_2\text{Se}_3$  thin films, we predict various topological and magnetic phases when the time-reversal symmetry is broken by magnetic ion doping. As the magnetic ion density increases, the system undergoes successive topological or magnetic phase transitions due to variation of the exchange field and the spin-orbit coupling. In order to identify the topological phases, we vary the spin-orbit coupling strength from zero to the original value of the system and count the number of band crossings between the conduction and valence bands, which directly indicates the change of the topological phase. This method provides a physically intuitive and abstract view to figure out the topological character of each phase and the phase transitions between them.

DOI: [10.1103/PhysRevB.84.134408](https://doi.org/10.1103/PhysRevB.84.134408)

PACS number(s): 75.70.-i, 73.20.At, 75.30.Kz

**I. INTRODUCTION**

Newly discovered topological insulators (TI) are differentiated from normal band insulators (BI) by the coexistence of a bulk band gap and gapless edge or surface states at the boundary.<sup>1-3</sup> The odd number of gapless surface states protected by time-reversal symmetry (TRS) show unique features such as spin chirality related to spin-momentum locking<sup>4</sup> and the absence of back-scattering by nonmagnetic impurities,<sup>5</sup> which make TI a promising candidate for spintronics applications. Combined with superconductivity or magnetism, TI have attracted great attention due to the rich variety of new physics and applications made possible; they provide, for example, topological magnetoelectric effects,<sup>6</sup> majorana zero modes,<sup>7</sup> and so on.

The quantum anomalous Hall (QAH) phase characterized by the quantized Hall conductance is another novel insulating phase derived from the combination of TI and magnetism. When the amount of TRS breaking field increases in the TI phase, the exchange field can kill the nontrivial topology of one spin channel, whereas the other channel remains as inverted band structures between the conduction and valence bands. Recently, the QAH phase was predicted in HgTe quantum wells, TI thin films, and graphene with magnetic impurities.<sup>8-10</sup>

In this work, we uncover the various phases induced by changing the concentration of the magnetic impurity in two-dimensional (2D) TI thin films. In the process of increasing the amount of magnetic dopants, we find magnetically and/or topologically different phases as well as the same phases from 2D TI, the so-called quantum spin Hall (QSH) and QAH states, for which the competition between the exchange field and spin-orbit coupling (SOC) is responsible. In order to identify each phase, we adopt the method proposed in Refs. 11 and 12, which studied the topological phase transition by varying external parameters, and expand it to the systems without TRS.

TI undergoes topological phase transitions as the SOC strength increases from 0 up to the real value of the system ( $\lambda_0$ ). At the transition point, a crossing between the conduction and valence bands occurs, resulting in the appearance of the Dirac cone in momentum space. The Dirac cone generates magnetic monopole-like Berry curvature, and its monopole charge, from integration of the field over the Brillouin zone, corresponds

to the quantized topological number. Due to the TRS, two Kramer's pairs of the conduction and valence bands are involved in the band crossing at the critical SOC strength. Once TRS breaking perturbations are introduced, the Kramer's degeneracy is split and topological phase transitions occur at two different SOC values. By counting the number of band crossing points within the range of the SOC strength from zero to  $\lambda_0$  or by tracing the two critical strengths, we can classify the topological and magnetic phases of the system and this is done here.

**II. COMPUTATIONAL DETAILS**

Bulk  $\text{Bi}_2\text{Se}_3$  has a rhombohedral crystal structure with space group  $D_{3d}^5$  ( $R3m$ ) with five atoms in a unit cell and a layered structure stacked along the  $c$  axis of the hexagonal lattice. One layer composed of five atoms is known as a quintuple layer (QL) and the interlayer coupling is due to the van der Waals interaction. The calculations are performed with the experimental lattice parameters of bulk  $\text{Bi}_2\text{Se}_3$  for the in-plane lattice constants and with full relaxation of the  $c$  axis and the internal coordinates. For magnetic doping, magnetic ions substitute for the outermost Bi atoms, and the inversion symmetry of the system is conserved for simplicity [see Fig. 1(a)]. To show the various topological phases by changing the exchange field strength, we vary the doping concentration or the atomic species of the magnetic ions (Cr and Fe). Variation of the magnetic ion concentration is determined by varying the supercell size. In Fig. 1(b), five different supercells are presented;  $1 \times 1$ ,  $\sqrt{3} \times \sqrt{3}$ ,  $2 \times 2$ ,  $\sqrt{7} \times \sqrt{7}$ , and  $\sqrt{12} \times \sqrt{12}$  configurations used for simulating the doping concentrations from 2.8% up to 33.3%.

To optimize the geometry, determine the electronic structures, and investigate the topological phase transition in 2D  $\text{Bi}_2\text{Se}_3$  films, we carried out first-principles electronic structure calculations using plane-wave basis and pseudopotentials within density functional theory. We employ the projector augmented wave pseudopotential<sup>13</sup> and the local density approximation<sup>14</sup> with on-site Coulomb interaction  $U$ <sup>15</sup> as implemented in the VIENNA *ab initio* simulation package.<sup>16</sup> For the localized  $3d$  orbitals of the magnetic ions,  $U_{\text{eff}} (=U - J)$  was set equal to 4.0 eV. To vary the SOC



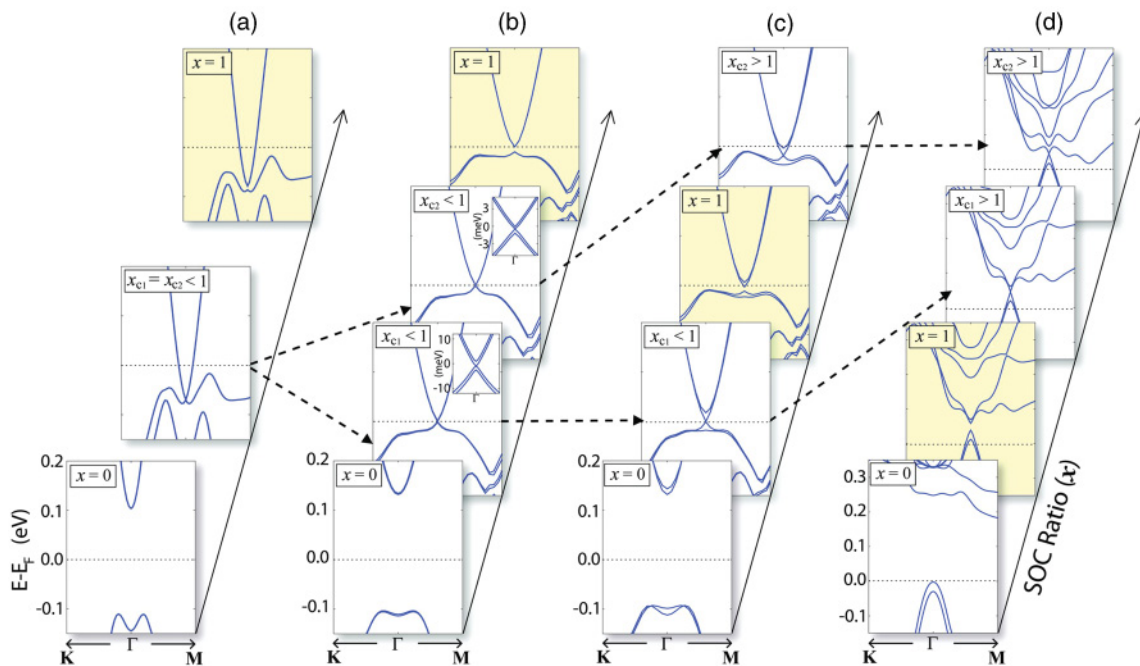


FIG. 3. (Color online) Band structures of the 3 QL  $\text{Bi}_2\text{Se}_3$  slab as a function of the SOC ratio  $x$  in (a) the pristine case, (b) 2.8% Cr doping, (c) 2.8% Fe doping, and (d) 33.3% Fe doping. The critical values of the SOC ratio are directly examined by gap closing: (a)  $x_{c1} = x_{c2} = 0.965$  for the pristine case, (b)  $x_{c1} = 0.944$  and  $x_{c2} = 0.949$  for 2.8% Cr doping, (c)  $x_{c1} = 0.878$  and  $x_{c2} = 1.055$  for 2.8% Fe doping, and (d)  $x_{c1} = 1.063$  and  $x_{c2} = 1.252$  for 33.3% Fe doping. Each configuration corresponds to (a) QSH with TRS, (b) QSH without TRS, (c) QAH, and (d) trivial FM phase, respectively. The evolution of the critical values are guided by the black dashed arrow. Insets of (b) are enlarged pictures near the Dirac point at two critical values.

number of edge states is the same. However, even though there are two counterpropagating edge states in the QSH without TRS phase, they are no longer time-reversal partners.

By maintaining the doping concentration but changing atomic species of Cr by Fe, we are able to increase the ferromagnetic moment by  $5\mu_B$  per Fe atom aligned along the  $c$  axis and the exchange splitting by 11.6 meV at the  $\Gamma$  point without SOC. Consequently, the QAH phase indicated by the condition  $x_{c1} < 1 < x_{c2}$  is realized in Fig. 3(c) ( $x_{c1} = 0.878$  and  $x_{c2} = 1.055$ ). Because  $x_{c2}$ , the second band crossing point, passes through 1 as the QSH evolves into the QAH phase when the exchange field grows, continuous deformation between the two phases without closing a gap is impossible, and the topological phase transition takes places. The QAH phase prevails over the range from 2.8% to 16.6% Fe doping in the 3 QL  $\text{Bi}_2\text{Se}_3$  slab, and the band gaps of the QAH phase are distributed from 6.9 meV (2.8%) to 39.1 meV (11.1%).<sup>26</sup>

Upon increasing the Fe density further, the system undergoes another topological phase transition; the 33.3% Fe doped 3 QL  $\text{Bi}_2\text{Se}_3$  film shows two critical values larger than 1 as shown in Fig. 3(d) ( $x_{c1} = 1.063$  and  $x_{c2} = 1.252$ ), designating the trivial ferromagnetic (FM) phase. Because there is no band crossing during the growth of the SOC ratio from 0 to 1, the electronic structure with full SOC strength is adiabatically connected to the  $x = 0$  state, which has a trivial topology. From QAH to trivial FM, the number of critical values smaller than 1 is altered; thus the transition is identified as a topological phase transition. This topological phase transition is not related to the increase of the exchange field, but is induced by the decrease

of the SOC strength because Fe has a much smaller SOC strength than Bi. Once we increase the doping concentration, the SOC strength of the system  $\lambda_0$  decreases simultaneously, making the first critical value  $x_{c1}$  larger than 1. To see the effect of the reduced SOC strength with excluding the influence of the exchange field, we calculated the hypothetical structure where every Fe atom in the trivial FM phase is replaced by As. The As-replaced system shows a trivial BI phase, i.e., two degenerate critical SOC ratios exceed 1, and this is indirect evidence that the QAH to trivial FM transition is mainly driven by reduction of the SOC strength.

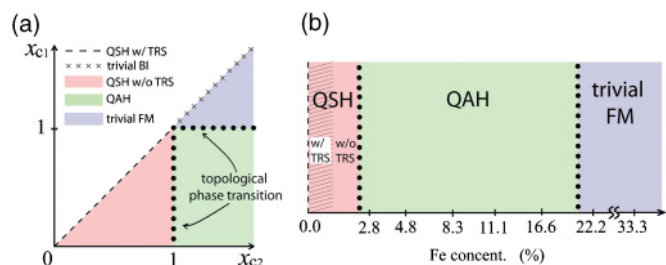


FIG. 4. (Color online) (a) Classification of each magnetic and topological phase in the  $(x_{c1}, x_{c2})$  plane and (b) the phase diagram on the 3 QL  $\text{Bi}_2\text{Se}_3$  slab. In (a), QSH with TRS, QSH without TRS, QAH, trivial FM, and BI phases are plotted as functions of critical values of the SOC ratio. In (b), QSH with TRS, QSH without TRS, QAH, and trivial FM phases are shown as the extent of magnetic doping increases.

Various phases identified by the range of the two critical SOC ratios,  $x_{c_1}$  and  $x_{c_2}$ , are sketched in Fig. 4(a). In this diagram, we assume that all phases, except for the critical line where the topological phase transition occurs ( $x_{c_1} = 1$  or  $x_{c_2} = 1$ ), are gapped and TRS is broken by the ferromagnetic ordering. Now the  $x_c$ 's are proportional to  $\Delta_{\text{gap}}/\lambda_0$ , where  $\Delta_{\text{gap}}$  is a bulk gap without SOC, and the difference between  $x_{c_1}$  and  $x_{c_2}$  is proportional to the exchange field. Therefore, the system with the SOC strength comparable to  $\Delta_{\text{gap}}$  and a moderate magnetic ion doping might be located around  $x_{c_1} = x_{c_2} = 1$  where the five different phases overlap, and easily show successive phase transitions by a small external perturbation.

The phase diagram of the 3 QL  $\text{Bi}_2\text{Se}_3$  thin film as a function of Fe concentration is depicted in Fig. 4(b). Upon increasing the Fe content, a magnetic phase transition occurs within the QSH phase, and then two topological phase transitions from QSH to QAH, and from QAH to trivial FM follow. The driving force for the first two transitions is the increase of the exchange field and the last one originates from the reduced SOC strength. From the competition between the exchange splitting and the SOC strength, the QAH phase is bounded, and the phase boundary is located near the 22.2% Fe doping concentration whose  $x_{c_1}$  is very close to 1 ( $x_{c_1} = 1.005$ ). The shaded area of the QSH with TRS phase considers the onset of ferromagnetic long-range ordering of the Fe impurities, which seems easily accessible according to the previous study.<sup>9,27</sup>

#### IV. CONCLUSION

We presented various topological and magnetic phases and the transitions between them in the 3 QL  $\text{Bi}_2\text{Se}_3$  thin film with magnetic impurities. Each phase is described by means of two critical SOC ratios, which provide intuitive understanding of the topological phase transition accompanied by the magnetic transition. Because the topological phases of the 2D systems are directly related to the existence and the character of the conducting edge states, it would be interesting to investigate the evolution of the edge states as the amount of the magnetic ion doping changes. In the QAH phase, the propagating direction of the edge state carrying the quantized Hall currents is coupled to the direction of the ferromagnetic moments of the magnetic impurities. Thus the Hall currents are able to be manipulated by flipping the ferromagnetic moments using an external magnetic field. Moreover, the 2D heterostructure or the multidomain structures containing different Fe densities could show a rich variety of interesting features, such as various topological phase domains and the conducting boundary states, and they might be applicable to electronic and spintronic devices using various 1D conducting channels.

#### ACKNOWLEDGMENTS

Support from the US DOE under Grant No. DE-FG02-88ER45372 is gratefully acknowledged.

\*h-jin@northwestern.edu

†j-im@northwestern.edu

- <sup>1</sup>M. Z. Hasan and C. L. Kane, *Rev. Mod. Phys.* **82**, 3045 (2010).
- <sup>2</sup>X. L. Qi and S. C. Zhang, e-print [arXiv:1008.2026v1](https://arxiv.org/abs/1008.2026v1) (unpublished).
- <sup>3</sup>J. E. Moore, *Nature (London)* **464**, 194 (2010).
- <sup>4</sup>D. Hsieh *et al.*, *Nature (London)* **460**, 1101 (2009).
- <sup>5</sup>P. Roushan *et al.*, *Nature (London)* **460**, 1106 (2009).
- <sup>6</sup>X.-L. Qi, R. Li, J. Zang, and S.-C. Zhang, *Science* **323**, 1184 (2009).
- <sup>7</sup>L. Fu and C. L. Kane, *Phys. Rev. Lett.* **100**, 096407 (2008).
- <sup>8</sup>C.-X. Liu, X.-L. Qi, X. Dai, Z. Fang, and S.-C. Zhang, *Phys. Rev. Lett.* **101**, 146802 (2008).
- <sup>9</sup>R. Yu *et al.*, *Science* **329**, 61 (2010).
- <sup>10</sup>Z. Qiao, S. A. Yang, W. Feng, W.-K. Tse, J. Ding, Y. Yao, J. Wang, and Q. Niu, *Phys. Rev. B* **82**, 161414 (2010).
- <sup>11</sup>S. Murakami and S.-I. Kuga, *Phys. Rev. B* **78**, 165313 (2008).
- <sup>12</sup>H. Jin, J.-H. Song, A. J. Freeman, and M. G. Kanatzidis, *Phys. Rev. B* **83**, 041202 (2011).
- <sup>13</sup>P. E. Blöchl, *Phys. Rev. B* **50**, 17953 (1994).
- <sup>14</sup>D. M. Ceperley and B. J. Alder, *Phys. Rev. Lett.* **45**, 566 (1980).
- <sup>15</sup>A. I. Liechtenstein, V. I. Anisimov, and J. Zaanen, *Phys. Rev. B* **52**, R5467 (1995).
- <sup>16</sup>G. Kresse and J. Furthmüller, *Phys. Rev. B* **54**, 11169 (1996).

- <sup>17</sup>D. J. Thouless, M. Kohmoto, M. P. Nightingale, and M. den Nijs, *Phys. Rev. Lett.* **49**, 405 (1982).
- <sup>18</sup>J. E. Avron, R. Seiler, and B. Simon, *Phys. Rev. Lett.* **51**, 51 (1983).
- <sup>19</sup>In these inversion-symmetric systems, conduction and valence bands exchange their parities at the crossing point.
- <sup>20</sup>Y. Xia *et al.*, *Nat. Phys.* **5**, 398 (2009).
- <sup>21</sup>H. Zhang *et al.*, *Nat. Phys.* **5**, 438 (2009).
- <sup>22</sup>Y. Zhang *et al.*, *Nat. Phys.* **6**, 584 (2010).
- <sup>23</sup>C.-X. Liu, H. J. Zhang, B. Yan, X.-L. Qi, T. Frauenheim, X. Dai, Z. Fang, and S.-C. Zhang, *Phys. Rev. B* **81**, 041307 (2010).
- <sup>24</sup>C. L. Kane and E. J. Mele, *Phys. Rev. Lett.* **95**, 226801 (2005).
- <sup>25</sup>M. König *et al.*, *Science* **318**, 766 (2007).
- <sup>26</sup>Our system is composed of 3 QL  $\text{Bi}_2\text{Se}_3$ , which is in the ultrathin limit and can be considered close to the 2D objects. The conduction and valence bands in these thin films, which are originally the two surface states from each surface, spread over the 3 QL. In the 11.1% doping configuration, we have checked the position dependence of the Fe dopants, and still found out the QAH phase for all three different locations. It is expected that the position dependence of the magnetic ions might be crucial for the thick film geometry. Considering the 2–3 nm spread of the surface states, the position dependence might emerge above 5 or 6 QL films.
- <sup>27</sup>L. A. Wray *et al.*, *Nat. Phys.* **7**, 32 (2011).